Journal of Sound and Vibration (1999) **227**(5), 915–933
Article No. jsvi.1999.2060, available online at http://www.idealibrary.com on IDEAL®

EVOLUTION OF RAIL CORRUGATION PREDICTED WITH A NON-LINEAR WEAR MODEL

J. B. NIELSEN

DSB – Development Office, Otto Bussesvej 5A, DK-2450 København SV
Dept. of Mathematical Modelling, Technical University of Denmark, DK-2800 Lyngby, Denmark

(*Accepted* 22 *September* 1998)

In the present work a non-linear wear model for the contact between a cylinder rolling over a periodically varying surface is derived. The model is a pure contact model where the dynamics of cylinder and surface are neglected. With the aid of the derived model it can be shown, that even if the normal force, the traction and the creep are held constant, corrugation will evolve due to the non-linearities of the contact mechanics. The model furthermore predicts the critical wave lengths for which the corrugation grows, and for which an initial corrugation is levelled out. Finally it is shown that the amplitude of the corrugation grows exponentially with a growth rate that for a given corrugation can be determined analytically.

1. INTRODUCTION

The evolution of rail corrugation is a large problem in railway traffic. Corrugation appears as a pattern of shortwave ripples along the surface of the rail, which generates noise and causes wear on the material and discomfort for the passengers. The typical wave length for short pitch corrugation lies within the range 0·03–0·1 m with wave amplitudes of magnitudes up to 100 μm. A thorough description of the various types of corrugation has been given by Grassie and Kalousek [1].

Although the problem has been known and investigated for many years, a fully satisfactory explanation of the phenomenon has not yet been found. Since the corrugation evolves over thousands of train passages experimental investigations are very difficult to carry out. Instead numerical simulations have become a powerful tool in the search for understanding of the evolution of corrugation. An overview of the different approaches has been given in the state of the art review by Knothe and Grassie [2].

Most of the corrugation models are focussed on the dynamics of wheel and rail with more or less primitive approximations then being applied for the contact mechanics. The excitation of the wheel and rail due to surface

0022–460X/99/450915 + 19 $30.00/0

irregularities or varying external parameters make the normal load and the traction oscillate. This oscillation is then considered as the reason for the evolution of the surface irregularities and thus the formation of corrugation. There is no doubt that this mechanism has an important influence on the growth of corrugation, but a result of the simplifications of the contact mechanics is that important properties of the wheel/rail interaction are neglected.

The present work is aimed at explaining the formation and evolution of corrugation from a pure contact mechanics point of view. This is done by neglecting the eigenforms and eigenfrequencies of the bodies in contact and including only the contact mechanics in the calculation of the wear. Surely the dynamics of the rail and wheel must be taken into account in a complete corrugation model, but in the present work it will be shown that a fully non-linear model of the contact mechanics itself influences the corrugation heavily and must be included in the ordinary simulation programs in order to yield more realistic results.

2. THE PHYSICAL SYSTEM

To investigate the influence of pure contact mechanics on the evolution of corrugation the two dimensional case of a cylinder rolling over a surface is examined (Figure 1). It is assumed that the level of the surface at any time can be described by a series of harmonic functions

$$Z(x) = \sum_{m=1}^{M} A_m \cos(k_m x) + B_m \sin(k_m x). \tag{1}$$

To simplify the model it is assumed that the entire wear is laid upon the surface, and so the cylinder will always have the constant radius R. This is reasonable as the model is intended to simulate many wheels running over the same surface.

If the curvature of the surface is larger than the curvature of the cylinder, a two point contact arises. This implies sudden shifts in the location of the contact point and the rolling motion is replaced by impacts between cylinder and surface. As this is the case only for heavily corrugated rails and thus of minor interest for the investigations of the formation of corrugation, the present model is confined only to the case of single point rolling contact. Thus it is assumed that the curvature of the cylinder is always much larger than the curvature of the surface: i.e.,

$$\sqrt{A_m^2 + B_m^2} R k_m^2 \ll 1, \qquad m = 1, 2, \cdots, M. \tag{2}$$

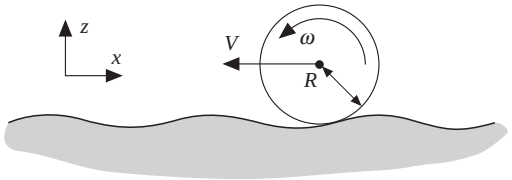

Figure 1. Cylinder rolling over a periodically varying surface.

Much work has been carried out to treat the case of multiple contact points (see, e.g. references [3] and [4]) where the configuration of an equivalent contact patch is derived from the actual contact patches. As the present work will show, the evolution of corrugation is very sensitive to what happens in the contact patch, and so those approximations are not well suited for wear calculations.

3. CONTACT MECHANICS

When two elastic bodies are pressed together under a normal load, they deform around their mutual contact point and a contact patch is created. In the case of wheel/rail contact the deformations of the bodies are small, and so the linear small strain theory can be applied [5]. As the size of the contact patch is much smaller than the characteristic sizes of wheel and rail the bodies can furthermore be considered as half spaces. The theory of half spaces has been described by Johnson [6].

3.1. THE NORMAL CONTACT PROBLEM

Let the height of the two undeformed bodies in the vicinity of the contact point be described by the functions $Z_1(\eta)$ and $Z_2(\eta)$ where η is a local position co-ordinate. Then the constitutive equation of Cerruti–Boussinesq yields a relation between the shape of the surfaces and the normal stress distribution $p(\eta)$ over the contact length $2a_0$ [6]:

$$-\frac{4(1-\nu^2)}{\pi E}\int_{-a_0}^{a_0}\frac{p(\bar{\eta})}{\eta-\bar{\eta}}\,\mathrm{d}\bar{\eta} = -\frac{\mathrm{d}}{\mathrm{d}\eta}(Z_1(\eta)-Z_2(\eta)), \qquad -a_0 \leqslant \eta \leqslant a_0. \tag{3}$$

Here E is the modulus of elasticity and ν is the Poisson's ratio. In the present work it is assumed that the two bodies are quasi-identical: i.e., have the same material properties. If this is not the case equivalent material properties for the system can be applied [7].

It is important to notice that the shapes of the surfaces are represented linearly in equation (3). This implies that roughness from one surface can be superposed on the other, and so any contact situation can be transformed into a contact between two surfaces where one of them is level.

The solution of the normal contact problem in the case of a cylinder rolling over a level surface was found by Hertz in 1882 [8]. In this case the shapes of the two bodies in contact are

$$Z_1(\eta) = R - \sqrt{R^2-\eta^2}, \qquad Z_2(\eta) = 0. \tag{4, 5}$$

Hertz made the assumption that the length of the contact patch is much smaller than the radius of the cylinder, and so the second order approximation of the cylinder,

$$Z_1(\eta) \simeq (1/2R)\eta^2, \qquad \eta \ll R, \tag{6}$$

can be applied. With this inserted in equation (3) the integral equation can be solved with respect to $p(\eta)$ and so it is found that the normal stress distribution over the contact patch is elliptic:

$$p(\eta) = E/[4(1-\nu^2)R]\sqrt{a_0^2 - \eta^2}, \qquad -a_0 \leqslant \eta \leqslant a_0. \tag{7}$$

As the normal load N is equal to the normal stress integrated over the entire contact patch the value of a_0 can be found as a function of N and R:

$$N = \int_{-a_0}^{a_0} p(\eta)\, \mathrm{d}\eta\, a_0 = \sqrt{8(1-\nu^2)RN/\pi E}. \tag{8}$$

To simplify the expression for the normal stress distribution, the maximum normal stress $p_0 = p(0)$ is introduced, and then the normal stress distribution becomes,

$$p(\eta) = (p_0/a_0)\sqrt{a_0^2 - \eta^2}, \quad -a_0 \leqslant \eta \leqslant a_0, \qquad p_0 = \sqrt{NE/2(1-\nu^2)\pi R}. \tag{9, 10}$$

3.2. THE TANGENTIAL CONTACT PROBLEM

If an axial torque is applied to the cylinder then a tangential force will interact between the two bodies, and the cylinder will roll over the surface. As a result of the compression of material in the contact patch the global relative velocity—the creep—between cylinder and surface is not necessarily zero. The creep is defined as

$$\xi = (V - \omega R)/\tfrac{1}{2}|V + \omega R|, \tag{11}$$

where ω is the angular velocity of the cylinder and V is the rolling velocity of the cylinder (see Figure 1). The local relative velocity $s(\eta)$ between the bodies is defined as

$$s(\eta) = \xi + \partial u/\partial \eta - (1/V)\partial u/\partial t, \tag{12}$$

where $u(\eta, t)$ is the tangential displacement of the material in the contact zone. If one assumes that $\partial u/\partial t$ is very small the constitutive equation for $\partial u/\partial \eta$ yields

$$s(\eta) = \xi - \frac{4(1-\nu^2)}{\pi E}\int_{-a_0}^{a_0} \frac{q(\bar{\eta})}{\eta - \bar{\eta}}\, \mathrm{d}\bar{\eta}, \tag{13}$$

where $q(\eta)$ is the tangential stress distribution over the contact patch.

The omission of the non-stationary term $\partial u/\partial t$ is evidently critical especially when the characteristic wave length of the corrugation is small relative to the length of the contact patch. Actually it is not possible to solve the non-stationary tangential problem for the two dimensional case as the value of $\partial u(0, t)/\partial t$ depends on the choice of the datum for the displacements. The problem of the non-stationary two dimensional contact problem has been described by Kalker [9]. The error introduced by neglecting the non-stationarity consists of an

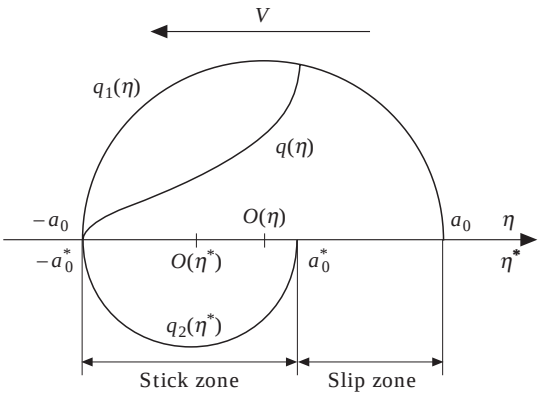

Figure 2. The Carter solution for the tangential stress distribution $q(\eta)$ for a cylinder rolling over a level surface.

oscillating term which must be added to the stationary creep. The amplitude of this term depends on the unknown $\partial u(0, t)/\partial t$.

The stationary tangential problem was solved by Carter in 1926 [10], who found that the tangential stress distribution can be evaluated as the sum of two ellipses. A new co-ordinate system, where the relation between the old and the new co-ordinate system is

$$\eta^* = \eta + a_0 - a_0^*, \tag{14}$$

is introduced. One of the ellipses then has its centre in $O(\eta)$ and the other in $O(\eta^*)$ as is indicated in Figure 2, and so the tangential stress distribution $q(\eta)$ is

$$q(\eta) = q_1(\eta) + q_2(\eta^*), \tag{15}$$

$$q_1(\eta) = \left\{ \begin{matrix} (\mu p_0/a_0)\sqrt{a_0^2 - \eta^2}, & -a_0 \leqslant \eta \leqslant a_0 \\ 0, & \text{otherwise} \end{matrix} \right\}, \tag{16}$$

$$q_2(\eta^*) = \left\{ \begin{matrix} -(\mu p_0/a_0)\sqrt{a_0^{*2} - \eta^{*2}}, & -a_0^* \leqslant \eta^* \leqslant a_0^* \\ 0, & \text{otherwise} \end{matrix} \right\}, \tag{17}$$

where μ is the friction coefficient. By inserting this tangential stress distribution into equation (13) the local relative velocity $s(\eta)$ between the bodies is found to be

$$s(\eta^*) = \left\{ \begin{matrix} 0, & -a_0^* \leqslant \eta^* \leqslant a_0^* \\ (\mu/R)\sqrt{\eta^{*2} - a_0^{*2}}, & a_0^* \leqslant \eta^* \leqslant 2a_0 - a_0^* \end{matrix} \right\}. \tag{18}$$

This implies that the contact patch is divided into a stick zone with the length $2a_0^*$ at the leading edge and a slip zone at the trailing edge (see Figure 2). In the stick zone $s(\eta) = 0$ while $s(\eta) \neq 0$ in the slip zone. The size of a_0^* depends on the

size of the contact length and the size of the creep:

$$a_0^* = a_0 - (R/\mu)\xi, \qquad 0 \leqslant \xi \leqslant \mu a_0/R. \tag{19}$$

The Carter solution and thus the Hertzian theory is the theory commonly used for two dimensional bodies in rolling contact. The problem however is that the theory of Hertz is based on a second order Taylor expansion of the bodies. This means that the bodies in the vicinity of the contact point must be described as

$$Z(\eta) = \alpha_0 + \alpha_1\eta + \alpha_2\eta^2. \tag{20}$$

When the surface is level, this yields of course the exact shape, but for a corrugated surface where the size of the characteristic wave length is small compared to the length of the contact patch, the second order approximation is too primitive. In this case it is necessary to use a higher order Taylor expansion of the surface.

3.3. A MORE REALISTIC APPROACH

In the following it is assumed that the accuracy of the second order approximation of the cylinder is still sufficient and thus that the size of the contact patch relative to the radius of the cylinder remains small even when the surface is corrugated. This is true due to the assumption from equation (2). For the corrugated surface the complete Taylor expansion is utilized. A relatively small order of the polynomial approximation of the harmonic functions will of course yield a fairly accurate result as the size of the contact patch is bounded, but as it turns out that the fully developed Taylor expansion gives closed form expressions for the size of the contact patch and the size of the stick zone, the cylinder and the corrugated surface will be described by the expressions

$$Z_1(\eta) = (1/2R)\eta^2, \tag{21}$$

$$Z_2(\eta) = \sum_{m=1}^{M} A_m \cos[k_m(Vt+\eta)] + B_m \sin[k_m(Vt+\eta)] = \sum_{i=0}^{\infty} \alpha_i \eta^i. \tag{22}$$

These are inserted into equation (3) which then must be solved with respect to $p(\eta)$. It can be shown that if

$$\int_{-a}^{a} \frac{h(\bar{\eta})}{(\eta-\bar{\eta})\sqrt{a^2-\bar{\eta}^2}}\,\mathrm{d}\bar{\eta} = \sum_{i=0}^{M} \gamma_i \eta^i, \qquad -a \leqslant \eta \leqslant a, \tag{23}$$

then the function $h(\eta)$ is a polynomial where the coefficients depend linearly on the γ_i's. This implies that the normal stress distribution for the case of a cylinder rolling over a harmonically varying surface has the form

$$p(\eta) = \frac{p_0}{a_0}\frac{\sum_{i=0}^{\infty} C_i \eta^i}{\sqrt{a^2-\eta^2}}, \qquad -a \leqslant \eta \leqslant a. \tag{24}$$

The coefficients C_i are defined so that

$$\sum_{i=0}^{\infty} C_i(-a)^i = \sum_{i=0}^{\infty} C_i(a)^i = 0, \tag{25}$$

which ensures that singularities in the normal stress distribution do not occur. Since the size of the contact patch is finite, η is bounded and as C_i tends very rapidly towards zero for large i's the normal stress distribution will always be bounded even though it is defined by an infinite series.

As a result of the asymmetries of the surface, the geometric contact point is no longer constantly located on the vertical projection of the cylinder axis. When the cylinder rolls downhill, the contact will take place behind the cylinder axis whereas the contact point is ahead of the cylinder axis when the cylinder rolls uphill. This mechanism is well known and included in many contact models. The asymmetric surface will however also cause the contact point not to be located in the centre of the contact patch. Instead the position of the centre is shifted the distance $\Delta(x)$ from the position of the cylinder axis

$$\Delta(x) = \sum_{m=1}^{M} Rk_m \mathrm{J}_0(a_0 k_m)[B_m \cos(k_m x) - A_m \sin(k_m x)]. \tag{26}$$

Here J_0 is the Bessel function of the first kind of order zero. Since the sign of $\mathrm{J}_0(a_0 k_m)$ varies, the size of $a_0 k_m$ influences on whether the centre of the contact patch is ahead of the cylinder axis or behind the cylinder axis.

So the shape of the surface compensates to some extent for the shift in the location of the contact point. The real contact length $2a$ is found as in the Hertzian case by integrating the normal stress distribution and then isolating a:

$$a(x) = a_0 - \sum_{m=1}^{M} Rk_m \mathrm{J}_1(a_0 k_m)[A_m \cos(k_m x) B_m \sin(k_m x)]. \tag{27}$$

The locations of the geometric contact point and the centre of the real contact patch are illustrated in Figure 3. It is seen that for the given contact configuration there is hardly any difference between the centre of the contact patch and the axis of the cylinder. As the location of the contact point depends only on the geometry of the bodies whereas the contact length and thus the normal load is included in $\Delta(x)$ it is not possible to make general conclusions with respect to the position of the contact point versus the centre of the contact patch. The assumption from equation (2) yields however that the centre of the contact patch will be located very close to the position of the cylinder axis.

A further important thing to notice is that the normal stress distribution is no longer elliptic. Due to the shape of the surface the symmetry of the stress distribution is broken down. It will later be shown that this asymmetric behaviour plays a very important role in the formation of the corrugation.

The above derived normal stress yields a tangential stress distribution equivalent to that of the Carter solution, with the slight change that the elliptic

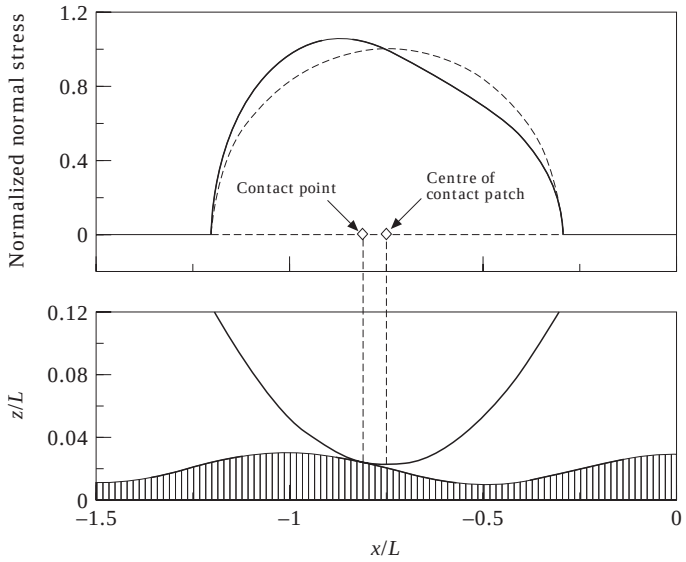

Figure 3. The location of the geometric contact point and the centre of the contact patch: – – – –, the Hertzian normal stress distribution; ———, the normal stress distribution for the fully developed Taylor expansion.

shape is replaced by a polynomial form:

$$q(\eta) = q_1(\eta) + q_2(\eta^*), \tag{28}$$

$$q_1(\eta) = \left\{ \begin{array}{cc} \dfrac{\mu p_0}{a_0} \displaystyle\sum_{i=0}^{\infty} C_i \eta^i / \sqrt{a^2 - \eta^2}, & -a \leqslant \eta \leqslant a \\ 0, & \text{otherwise} \end{array} \right\}, \tag{29}$$

$$q_2(\eta^*) = \left\{ \begin{array}{cc} \dfrac{-\mu p_0}{a_0} \displaystyle\sum_{i=0}^{\infty} C_i^* \eta^{*i} / \sqrt{a^{*2} - \eta^{*2}}, & -a^* \leqslant \eta^* \leqslant a^* \\ 0, & \text{otherwise} \end{array} \right\}, \tag{30}$$

Similarly the local relative velocity is found to be

$$s(\eta^*) = \left\{ \begin{array}{cc} 0, & -a^* \leqslant \eta^* \leqslant a^* \\ \dfrac{\mu}{R} \displaystyle\sum_{i=0}^{\infty} C_i^* \eta^{*i} / \sqrt{\eta^{*2} - a^{*2}}, & a^* \leqslant \eta^* \leqslant 2a - a^* \end{array} \right\}. \tag{31}$$

The size of the stick zone a^* is no longer constant in time but can be calculated

as

$$a^*(x) = a_0^* - \Delta(x) + a(x) - a_0 + \sum_{n=1}^{N} Rk_m \mathrm{J}_0(a_0^* k_n)[B_m \cos(k_m(x - a_0 + a_0^*)) - A_m \sin(k_m(x - a_0 + a_0^*))]. \tag{32}$$

This yields that the size of the stick zone oscillates with the same wave length as the size of the entire contact patch, but the phase and the amplitude of the oscillation are different.

The Carter solution and the solution with a fully developed Taylor expansion of the surface are given for four different contact situations in Figures (4a–d). Some qualitative differences between the two approaches must be emphasized. As stated earlier the centre of the contact patch is—as a result of the geometry of the bodies—no longer constantly located on the vertical projection of the cylinder axis. Secondly the size of the contact patch and the size of the slip zone change as the cylinder rolls over the corrugated surface. These two changes in the contact configuration are however not crucial as their amplitudes are small and so they will not make a significant impact on the evolution of the corrugation.

Far more important is the asymmetry in the normal stress distribution which is transmitted to the tangential stress distribution. This implies that the contribution from the slip zone to the entire tangential force oscillates with a rather large amplitude as the cylinder rolls over the surface. Since the wear is generated in the slip zone this oscillation will be transformed into the wear. So even when the cylinder rolls over the surface with a constant normal force and a constant tangential force the corrugation can evolve because the size of the tangential stress in the slip zone varies.

4. WEAR

The wear of the surface is caused by the tangential force between the bodies in contact and is defined as the height of material removed from the surface after one passage of the cylinder. The wear is proportional to the frictional work density [11],

$$W(x) = KV \int q(x, t)s(x, t)\, \mathrm{d}t, \tag{33}$$

where V is the velocity of the cylinder and K is a material dependent constant. An often seen simplification of this expression is the linearized form

$$W(x) = KT(x)\xi(x), \tag{34}$$

where $T(x)$ is the tangential force and $\xi(x)$ is the creep due to the Carter solution i.e., the global relative velocity (equation (11)). This approximation however implies that the wear over the surface is constant if the tangential force and the

creep are kept constant, which contradicts the arguments from the previous section. Instead the integral must be solved for the fully developed solution to the tangential contact problem derived in the previous section.

4.1. CALCULATING THE WEAR

The integral in equation (33) for the more realistic approach from section 3.3 is

$$W(x) = KV \int_{2a^*-a}^{a} \frac{\mu p_0}{a_0} \frac{\sum_{i=0}^{\infty} C_i \eta^i}{\sqrt{a^2 - \eta^2}} \frac{\mu}{R} \frac{\sum_{i=0}^{\infty} C_i^* \eta^{*i}}{\sqrt{\eta^{*2} - a^{*2}}} \, \mathrm{d}t, \tag{35}$$

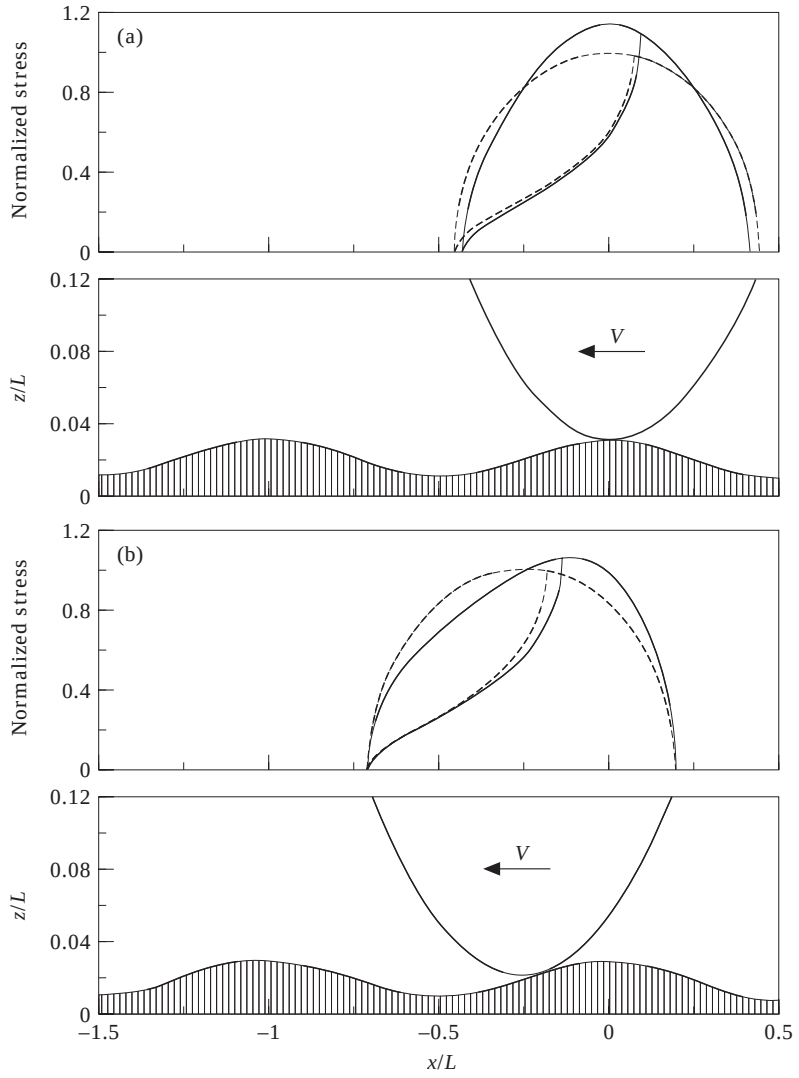

Figure 4. Stress distribution for a cylinder rolling over a periodically varying surface. Top: tangential stress distribution for the Carter approximation (– – – –) and for the solution based on fully developed Taylor expansions (———). Bottom: the cylinders position on the surface. (a) $Vt = 0$; (b) $Vt = -L/4$; (c) $Vt = -L/2$; (d) $Vt = -3L/4$.

which can be calculated to yield

$$W(x) = (KVN/R)[\mu C_0(x)/a(x)]^2 \tau(x)[1 - r_\tau(x) - r_\tau^2(x) + r_T^3(x)], \tag{36}$$

$$r_\tau(x) = \tau^*(x)/\tau(x), \tag{37}$$

where $\tau(x)$ is half the time it takes for the entire contact patch to pass the position x and $\tau^*(x)$ is half the time it takes the stick zone to pass x.

This leads for the surface

$$Z(x) = A\cos(kx) + B\sin(kx) \tag{38}$$

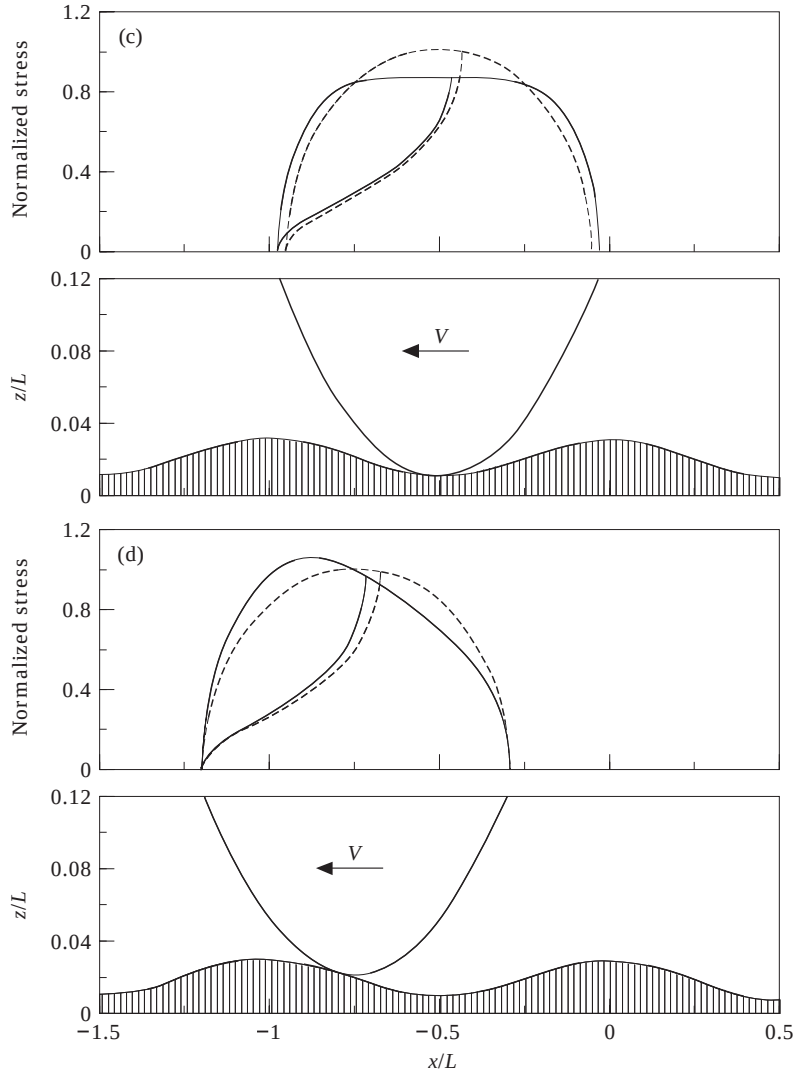

Figure 4. (continued)

to the following expression for the wear:

$$W(x) = W_0 + (W_1 A + W_2 B)\cos(kx) + (W_1 B - W_2 A)\sin(kx) + \mathcal{O}((A+B)^2). \tag{39}$$

With the assumption from equation (2) that the curvature of the cylinder is always much larger than the curvature of the surface all the higher order terms in equation (39) can be neglected. As it is the amplitude of the corrugation that is of major interest the constant term W_0 is also omitted, and so the actual wear after one passage of the cylinder can be approximated by

$$W(x) = (W_1 A + W_2 B)\cos(kx) + (W_1 B - W_2 A)\sin(kx), \tag{40}$$

where the wear coefficients W_1 and W_2 are given as

$$W_1 = K\mu^2 (N/a_0) f(ka_0, ka_0^*), \qquad W_2 = K\mu^2 (N/a_0) g(ka_0, ka_0^*). \tag{41, 42}$$

The two functions $f(ka_0, ka_0^*)$ and $g(ka_0, ka_0^*)$ are analytically given and involve harmonic functions and Bessel functions of the first kind of order zero and order one. Because the wear depends linearly on A and B, the nature of the wear is such that if the surface can be described by a series of harmonic functions (equation (1)) then the global wear is equal to the sum of the wear contributions from each of the harmonic functions:

$$Z(x) = \sum_{m=1}^{M} A_m \cos(k_m x) + B_m \sin(k_m x) \Rightarrow$$

$$W(x) = \sum_{m=1}^{M} (W_{m,1} A_m + W_{m,2} B_m)\cos(k_m x) + (W_{m,1} B_m - W_{m,2} A_m)\sin(k_m x). \tag{43}$$

In this way even the wear of a very complicated surface configuration can be found, simply by calculating the Fourier representation of the surface and then finding and summing up the wear for each term of the Fourier series.

5. EVOLUTION OF CORRUGATION

5.1. CALCULATING THE CORRUGATION

With the wear defined as the height of the material removed as the cylinder rolls over the surface, it is obvious that the shape of the surface after one passage of the cylinder is equal to the old surface minus the wear. This yields for the surface given in equation (38) and the corresponding wear (equation (40)) that

$$Z^{\{1\}}(x) = Z^{\{0\}}(x) - W^{\{0\}}(x) \Rightarrow Z^{\{1\}}(x) = A^{\{1\}}\cos(kx) + B^{\{1\}}\sin(kx), \tag{44}$$

where the high indices refer to the number of cylinder passages. So if the level of the initial surface is harmonic, then the level after one passage of the cylinder is also harmonic with the same wave length but with different amplitude and phase. This gives the discrete mapping

$$\begin{Bmatrix} A^{\{n+1\}} \\ B^{\{n+1\}} \end{Bmatrix} = \begin{bmatrix} 1 - W_1 & -W_2 \\ W_2 & 1 - W_1 \end{bmatrix} \begin{Bmatrix} A^{\{n\}} \\ B^{\{n\}} \end{Bmatrix} \tag{45}$$

From this discrete mapping it is possible to make a calculation of the shape of the surface after each passage of the cylinder in a completely straightforward analytical way. Thus time consuming integrations or space stepping are avoided, and so the present method is as fast as any other method based on more primitive models for the contact mechanics

5.2. AMPLIFYING AND LEVELLING ZONES

The fact that the development of the corrugation can be calculated by analytical, closed forms makes it possible to derive some qualitative properties concerning the evolution of the corrugation. From the discrete mapping introduced in the previous section (equation (45)) it is found that the amplitude of the surface after one passage of the cylinder can be described by the former surface configuration as

$$A^{\{n\}^2} + B^{\{n\}^2} = (1 - 2W_1)(A^{\{n-1\}^2} + B^{\{n-1\}^2}), \tag{46}$$

which is generalized to

$$A^{\{n\}^2} + B^{\{n\}^2} = (1 - 2W_1)^n (A^{\{0\}^2} + B^{\{0\}^2}). \tag{47}$$

This means that the growth rate of the corrugation depends only on the size of $(1 - 2W_1)$: if this term is smaller than 1 any initial amplitude will be levelled out whereas the amplitude grows exponentially if $(1 - 2W_1) > 1$. As $|W_1| \ll 1$ the criteria of stability are

$$\begin{aligned} &W_1 > 0 \Leftrightarrow \text{the corrugation is levelled out} \\ &W_1 < 0 \Leftrightarrow \text{the corrugation is amplified.} \end{aligned} \tag{48}$$

With the wave length of the corrugation introduced as $L = 2\pi/k$, then the sign of W_1 depends only on L/a_0 and a_0^*/a_0, and so these two ratios are crucial for the formation of corrugation. A typical outline of W_1 for a fixed a_0^*/a_0 value is given in Figure 5. This indicates that there exists one and only one critical L/a_0 ratio for which $(1 - 2W_1) = 0$. This is the limit of stability and so surface irregularities with L/a_0 ratio smaller than this value are levelled out while the corrugation is amplified if the L/a_0 ratio exceeds the critical value. Furthermore it is seen that $(1 - 2W_1)$ tends towards 1^+ for long wave lengths. This states that if the wave length of the corrugation is large compared with a_0 then the amplitude of the corrugation is unaffected by the contact mechanics.

In Figure 6 the qualitative evolution of a corrugated surface is shown. The initial surface consists of two different wave lengths L_1 and L_2 where L_1

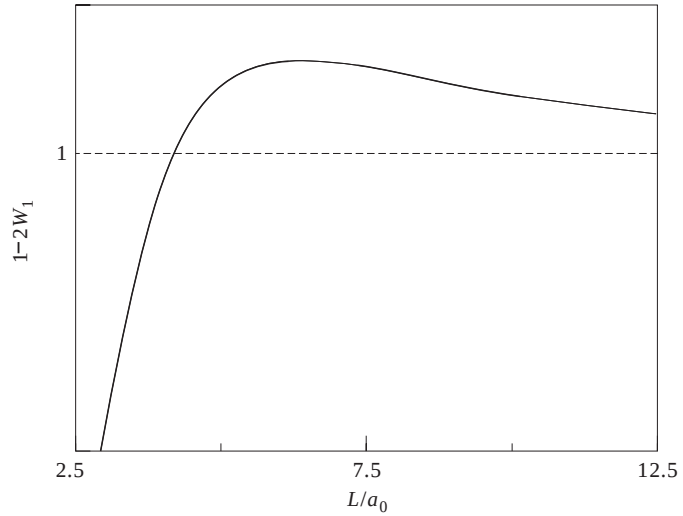

Figure 5. The wear coefficient $(1-2W_1)$ for $a_0^*/a_0 = 0{\cdot}6$.

is smaller than the critical wave length and L_2 is bigger than the critical wave length. As initial condition the amplitude belonging to L_1 is set to be 10 times larger than the amplitude belonging to L_2. It is seen that as the number of passages increases, the wave length which initially was dominant is levelled out while the other grows rapidly.

The critical wave length as a function of a_0^*/a_0 is shown in Figure 7. This line divides the $(a_0^*/a_0, L/a_0)$-space into an amplifying zone above the line and a levelling zone below the line. In this way the line represents the smallest possible wave lengths for which corrugation can occur.

So the deformations of the bodies act like a filter on the surface irregularities. It is not something new to apply a contact filter to take the filtering effect of the

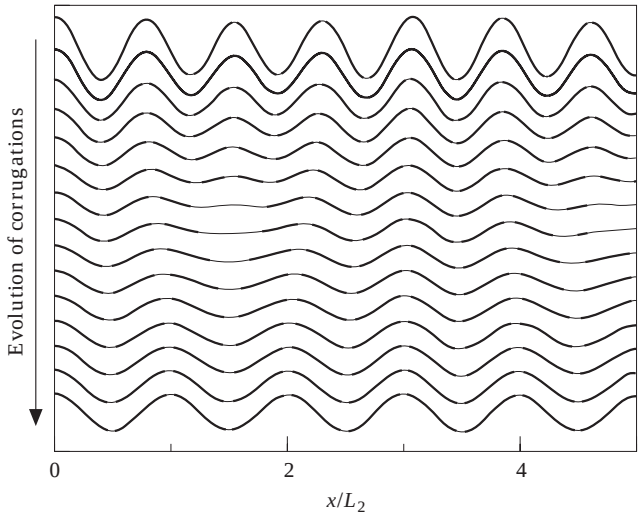

Figure 6. The qualitative evolution of corrugations.

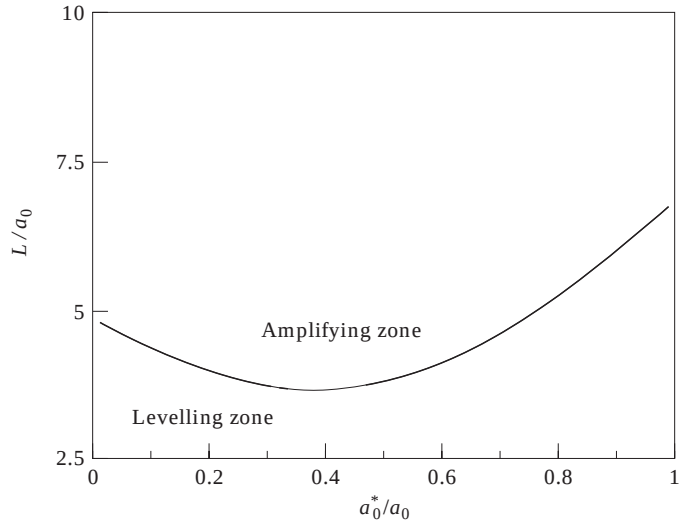

Figure 7. The smallest possible wave lengths of the corrugation.

size of the contact patch into account. One of the most frequently used filters was suggested by Remington [12] who introduced a contact filter for a rectangular contact patch:

$$F_{Remington} = \frac{L}{2\pi a_0} \sin(2\pi a_0/L). \tag{49}$$

This filter is not directly applicable to a wear problem as the negative values implies that the surface in these cases is coated with material as the cylinder passes by. To avoid this non-physical behaviour Hempelmann [13] has introduced a modified Remington contact filter where negative values do not occur. It is seen that the only critical value for the Remington filter is the L/a_0 ratio whereas the relative size of the stick zone is not included. This is a crucial lack of the Remington filter compared with the results obtained with the present model.

The qualitatively discrepancies between the Carter solution with a contact filter and the method described in this paper can be illustrated very easily. By introducing the equivalent radius $R_{equivalent}$ of the contact system as

$$1/R_{equivalent}(x) = 1/R_{cylinder} + 1/R_{surface}(x), \tag{50}$$

the Carter solution is found to depend on the position of the cylinder. With the assumption that the wear takes place in the centre of the slip zone this yields that

$$\begin{aligned} W_{Carter}(x) \simeq W_0 &+ (W_{1,\,Carter}\,A + W_{2,\,Carter}\,B)\cos(kx) \\ &+ (W_{1,\,Carter}\,B - W_{2,\,Carter}\,A)\sin(kx), \end{aligned} \tag{51}$$

$$W_{1,\,Carter} = -K\mu^2(N/a_0)(ka_0)^2 r_{a_0}(1 - 2r_{a_0} + r_{a_0}^2)\cos(ka_0^*)F_{Remington}, \tag{52}$$

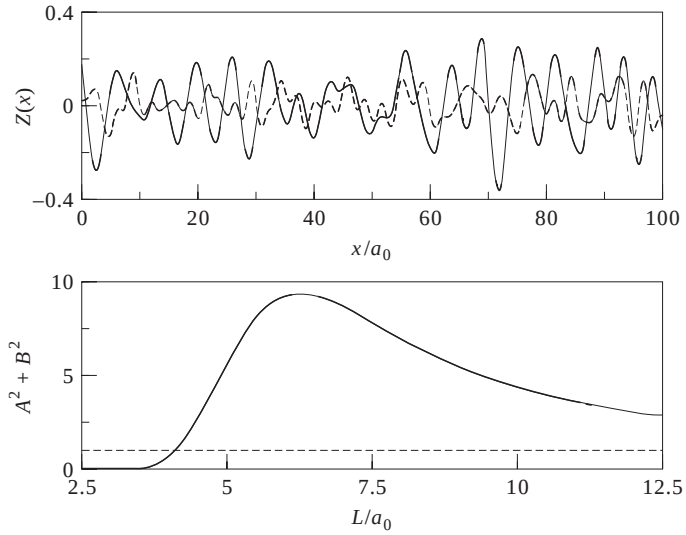

Figure 8. The evolution of initial surface irregularities represented by white noise. Top: level of the surface: – – – –, initial surface; ———, surface after a number of cylinder passages. Bottom: the spectra of the surface irregularities: – – – –, initial surface; ———, surface after a number of cylinder passages.

$$W_{2,\,Carter} = -K\mu^2(N/a_0)(ka_0)^2 r_{a_0}(1 - 2r_{a_0} + r_{a_0}^2)\sin(ka_0^*)F_{Remington}, \tag{53}$$

$$r_{a_0} = a_0^*/a_0. \tag{54}$$

Provided that the contact filter does not depend on a_0^* this implies that the limit between amplifying zone and levelling zone is given by

$$W_{1,\,Carter} = 0 \Rightarrow \cos(ka_0^*) = 0 \Rightarrow L/a_0 = 4a_0^*/a_0. \tag{55}$$

So with a contact filter applied to the Carter solution, the smallest possible wave length is found to be a linear relation between L/a_0 and a_0^*/a_0. This is in strong contrast to the result shown in Figure 7. It is evident from the above result that the asymmetry of the stress distribution is a very important factor in the formation of corrugation: the present method where the asymmetry is taken into account provides results quite different from the Carter solution combined with a contact filter.

5.3. CHARACTERISTIC WAVE LENGTH

Another important property is that $(1 - 2W_1)$ has a maximum. At first this maximum does not seem to be very dramatic, but because the wear rate is given as $(1 - 2W_1)^n$ a very distinct peak in the frequency spectra will grow up as the number of cylinder passages (n) increases. So this relative wave length will be dominating the corrugation, which explains why a certain corrugation pattern usually evolves with one and only one distinct wave length. This effect is seen in Figure 8 where the initial corrugation of the surface is given as white noise. After a number of cylinder passages a corrugation pattern with one dominant

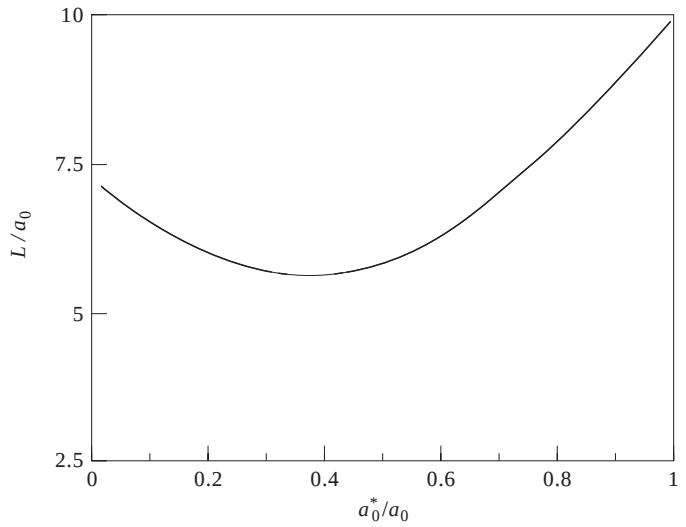

Figure 9. The characteristic wave lengths for which the corrugation is most likely to develop.

wave length has evolved. In practice broad spectra of wave lengths are always to some extent represented on the surface of a rail. Because the wave length is much more decisive for the evolution of the corrugation than the initial amplitude, this means that a certain characteristic wave length without any apparent reason will emerge even though it is not dominant in the initial wheel/rail system.

The characteristic wave length depends on the a_0^*/a_0 ratio and thus the magnitude of the creep. So if the creep changes, the characteristic wave length of the corrugation will change. In Figure 9 this characteristic wave length is shown for different a_0^*/a_0 values. It is seen that the L/a_0 ratio for the characteristic wave length lies in the range from 5–10. In wheel/rail contact the typical size of a_0 is somewhere between 5 mm and 10 mm, which thus provides a characteristic wave length in the interval 0·025–0·1 m. This fits very well with the observed wave lengths for short pitch corrugation [1].

As the principle of superposition is valid, the resulting wear rate after N passages with varying a_0^*/a_0 ratios can be calculated as

$$A^{\{N\}^2} + B^{\{N\}^2} = \left(\prod_{n=1}^{N} [1 - 2W_1(L/a_0^{\{n\}}, a_0^{*\{n\}}/a_0^{\{n\}})] \right) (A^{\{0\}^2} + B^{\{0\}^2}), \tag{56}$$

which makes it possible to find the peak in the frequency spectrum and thus the characteristic wave length after many different wheels with different creeps have rolled over the surface.

6. CONCLUSIONS

A non-linear wear model for a cylinder rolling over a periodically varying surface has been presented. By keeping all external parameters except the surface

level constant it is possible with this model to derive some of the basic qualities of wheel/rail interaction in order to explain the formation and evolution of rail corrugation. Three important results have been pointed out. First it is possible with a discrete mapping to calculate the wear and thus the evolution of initial surface irregularities. Secondly it has been shown, that an initial corrugation can either be amplified or levelled out depending on the sizes of L/a_0 and a_0^*/a_0. This yields that the $(a_0^*/a_0, L/a_0)$-space is divided into an amplifying zone and a levelling zone. The limit between these two zones is the smallest possible wave length of the corrugation. Finally the model can predict the characteristic wave length of the corrugation, a wave length that depends uniquely on the two ratios L/a_0 and a_0^*/a_0. The amplitude of the corrugation will grow exponentially with the number of cylinder passages.

In general the initial amplitudes of the surface irregularities are not crucial for the evolution of the corrugation. As the growth of the corrugation is exponential, the wave length of a surface component is far more important than the amplitude. In practice all wave lengths are to some extent represented on the surface of a rail, and as the corrugation pattern is wave length dependent the general pattern of the corrugation at two different places will evolve in the same way if the characteristics of the wheels rolling over it are the same. Similarly the evolution of the rail corrugation on an arbitrary rail can be predicted if only the distributions of the creep and the contact length of the passing wheels are known.

REFERENCES

1. S. L. Grassie and J. Kalousek 1993 *Proceedings of the Institution of Mechanical Engineers, Part F: Journal of Raid and Rapid Transit* **207**, 57–68. Rail corrugation: characteristics, causes and treatments.
2. K. Knothe and S. L. Grassie 1993 *Vehicle System Dynamics* **22**, 209–262. Modelling of railway track and vehicle/track interaction at high frequencies.
3. J. Piotrowsky 1982 *Vehicle System Dynamics* **11**, 69–87. A theory of wheelset forces for two point contact between wheel and rail.
4. J. P. Pascal and G. Sauvage 1991 *Proceedings of the* 12*th IAVSD-Symposium, Lyon*, 475–489. New method for reducing the multi-contact wheel/rail problem to one equivalent rigid contact patch.
5. S. Timoshenko and J. N. Goodier 1951 *Theory of Elasticity*. Tokyo: McGraw-Hill (3rd edition)
6. K. L. Johnson 1985 *Contact Mechanics*. Cambridge University Press.
7. J. J. Kalker 1990 *Solid Mechanics and its Applications* Three-dimensional elastic bodies in rolling contact. Dordrecht: Kluwer Academic Publisher (Volume 2).
8. H. Hertz 1882 *Journal für die reine und angewandte Mathematik* **92**, 156–171. Über die Berührung fester elastischer Körper.
9. J. J. Kalker 1971 *Journal of Applied Mechanics* **38**, 875–887. A minimum principle for the law of dry friction, with application to elastic cylinders in rolling contact, Parts 1, 2.
10. F. W. Carter 1926 *Proceedings of the Royal Society of London* **A112**, 151–157. On the action of a locomotive driving wheel.
11. A. Valdivia 1988 *VDI – Fortschrittsbericht*, **93**, *Reihe* 12; Düsseldorf: VDI Verlag. Die Wechselwirkung zwischen hochfrequenter Rad-Schiene-Dynamik und undgleichfömigem Schienenverschleiß – ein lineares Modell.

12. P. J. REMINGTON 1976 *Journal of Sound and Vibration* **46**, 359–451. Wheel–rail noise, Parts 1–IV.
13. K. HEMPELMANN 1995 *VDI-Fortschritt-Berichte* **231**, *Reihe* 12; Düsseldorf: VDI Verlag. Short pitch corrugation on railway rails—a linear model for prediction.